Unsteady Analysis of Inlet-Compressor Acoustic Interactions Using Coupled 3-D and 1-D CFD Codes

A. Suresh
Dynacs Engineering Company, Inc., Brook Park, Ohio

G.L. Cole
Glenn Research Center, Cleveland, Ohio

National Aeronautics and
Space Administration

Glenn Research Center

September 2000

Acknowledgments

UNSTEADY ANALYSIS OF INLET-COMPRESSOR ACOUSTIC INTERACTIONS USING COUPLED 3-D AND 1-D CFD CODES

A. Suresh
Dynacs Engineering Company, Inc.,
National Aeronautics and Space Administration
Glenn Research Center
Cleveland, Ohio 44135

G.L. Cole
National Aeronautics and Space Administration
Glenn Research Center
Cleveland, Ohio 44135

SUMMARY

It is well known that the dynamic response of a mixed compression supersonic inlet is very sensitive to the boundary condition imposed at the subsonic exit (engine face) of the inlet. In previous work, a 3-D computational fluid dynamics (CFD) inlet code (NPARC) was coupled at the engine face to a 3-D turbomachinery code (ADPAC) simulating an isolated rotor and the coupled simulation used to study the unsteady response of the inlet. The main problem with this approach is that the high fidelity turbomachinery simulation becomes prohibitively expensive as more stages are included in the simulation. In this paper, an alternative approach is explored, wherein the inlet code is coupled to a lesser fidelity 1-D transient compressor code (DYNTECC) which simulates the whole compressor. The specific application chosen for this evaluation is the collapsing bump experiment performed at the University of Cincinnati, wherein reflections of a large-amplitude acoustic pulse from a compressor were measured. The metrics for comparison are the pulse strength (time integral of the pulse amplitude) and wave form (shape). When the compressor is modeled by stage characteristics the computed strength is about 10 percent greater than that for the experiment, but the wave shapes are in poor agreement. An alternate approach that uses a fixed rise in duct total pressure and temperature (so-called "lossy" duct) to simulate a compressor gives good pulse shapes but the strength is about 30 percent low.

INTRODUCTION

CFD simulations are seeing an increasing role in predicting the unsteady response of mixed compression inlets to atmospheric and engine disturbances. The ability to predict the unsteady response is particularly important for evaluating the inlet unstart tolerance. A major uncertainty in these simulations is the boundary condition used at the exit of the inlet that tries to mimic the presence of the engine. Previously, a code coupling approach was used to shed some light on conditions at the inlet-engine interface.[1] In that study, a 3-D unsteady inlet code was coupled at the engine face with a 3-D turbomachinery code simulating an isolated rotor. While the initial portion of a reflected pulse obtained from the analysis compared well with experimental data, it appears that simulation of additional (if not all) stages is required to best match the pulse strength and shape measured in the experiment. However, extension of the turbomachinery simulation to include additional stages, including rotor-stator interactions, would be computationally prohibitive without considerable additional (parallel) computer resources.

In this work, we describe another approach to the problem. Several 1-D codes are now available that simulate the steady and transient flow through a complete compressor. These codes typically solve the 1-D steady and unsteady Euler equations with the effect of the blades being modeled by appropriate source terms in the momentum and energy equations. In this work, one such code (DYNTECC) is coupled dynamically to an unsteady inlet code and the coupled codes are used to study inlet-compressor interactions.

The potential advantage of such an approach is that the entire compressor can be included in the analysis for little more than the cost of a stand-alone inlet simulation.

This approach also has several limitations, the most obvious one being that 1-D codes cannot be used to analyze disturbances that are not predominantly 1-D in nature, such as a convective (tangential) velocity perturbation, which are sometimes important. However, even for axial disturbances, since inlet-engine interactions involve the reflection of acoustic waves from turbomachinery, it is not clear whether such 1-D codes will give meaningful results. On the one hand, since there is no blade surface, it is obvious that reflections from individual blades will not be captured. On the other hand, since the overall temperature and pressure rises are captured, these along with the area variation might give the correct reflected response far from the turbomachinery itself. More importantly, even if the reflected pulse is not completely accurate, the hope is that the coupled-component simulation might provide a better assessment of inlet unstart tolerance than the imposition of simple boundary conditions at the inlet exit.

The objectives of this work were threefold: 1) to evaluate the source term approach for representing the compressor stages, 2) to extend the analysis from the previous work[1] to include the complete compressor, and 3) to investigate 1-D to 3-D coupling which is required for the zooming capability of the Numerical Propulsion System Simulation (NPSS) project at the NASA Glenn Research Center. This report describes the experiment chosen for simulation and evaluation of the approach, the codes used to simulate the inlet and compressor components, and the code-coupling procedure. Results from several coupled-simulation cases are then discussed and compared to each other and to experimental results, followed by some concluding remarks.

DESCRIPTION OF EXPERIMENT

The collapsing-bump inlet-compressor experiment conducted at the University of Cincinnati[2] was chosen as the simulation application. The experimental setup is shown schematically in Fig. 1. It consists of a constant area annular inlet duct mated with a General Electric T58 engine modified for cold operation (i.e., the turbine was driven by an external air supply). The inlet duct is about 71 inches long and has a screened bellmouth at the upstream end. A small section of the constant area duct has a flexible bump on the hub surface that collapses rapidly (in about 1 msec) to produce two well-defined expansion waves or acoustic pulses, one traveling upstream and the other downstream. The length of duct upstream of the bump was chosen so that reflections of the upstream traveling pulse arrive at the measurement stations after the time interval of interest. The corresponding axial area distribution is shown in Fig. 2, where the normalizing factors Rc and Ac are 5.083 in. and 81.17 sq. in., respectively. The compressor is quite short and is seen to represent a fairly abrupt reduction in area.

In our computations, the long inlet duct with the bump was solved using NPARC, a general purpose CFD code capable of handling moving grids. The engine's compressor was modeled using DYNTECC, a 1-D transient compressor code.

INLET SIMULATION USING NPARC

The simulation of the collapsing bump using NPARC version 3.1[3] is very similar to that described in Ref. 1. Since viscous effects were not found to be significant, the flow was simulated as an inviscid 3-D flow. At the downstream end, where it is coupled with DYNTECC, the grid was modified so as to remove a converging section so that the flow remains one dimensional. This was done primarily to be consistent with the 1-D flow assumed in DYNTECC and also to eliminate a potential source of reflections. Although the flow is axisymmetric, it is solved here as a 3-D flow to permit investigation of 3-D to 1-D interface coupling.

The grid for the inlet simulation consists of 338 by 33 by 13 points in the axial, radial, and circumferential directions, respectively. The default ADI algorithm in NPARC is used to obtain the reference steady state

solution. Since the Mach number is quite low, the second order dissipation is set to zero in these computations. For the unsteady computations a Newton iterative method is used to iterate the steady state algorithm which allows for the use of larger time steps.

TURBOMACHINERY SIMULATION USING DYNTECC

GENERAL DESCRIPTION OF DYNTECC

DYNTECC[4,5] is a 1-D stage-by-stage compression system model developed at AEDC. It solves the 1-D steady/unsteady Euler equations, with source terms used to compute the effect of the blades. It has the capability to analyze post-stall behavior as well as predict the onset of system instability for any generic compression system as well as model the performance of the compressor under surge and rotating stall modes. In addition to the flow path geometry, a set of individual stage (rotor/stator pair) characteristics of the compression system is required as input. The magnitude of the source terms are calculated from these characteristic maps.

In addition to the input file, which contains user inputs that control various aspects of the simulation, two other files are required. The first is the .geom file that contains the flow path of the compressor. The T58 compressor has 10 stages and an IGV and OGV, as shown in Fig. 1. Typically, each stage is represented by a control volume. For each control volume, the axial location, hub and tip radii at the beginning and end of the control volume are required. This was obtained by digitizing the flow path geometry of the T58 engine.

Since DYNTECC does not have a nonreflecting boundary condition, a long uniform duct was added to the downstream end of the T58 compressor (Fig. 2) so that reflections from the constant-pressure exit boundary condition would not be present in the space-time interval of interest. A total of 40 grid points were used in the DYNTECC simulation, eleven of which were used in the compressor region.

GENERATION OF DYNTECC STAGE CHARACTERISTIC MAPS

A file (.fit file) that contains parametric fits that represent characteristic maps of each stage of the compressor is read by DYNTECC prior to execution. The usual way of obtaining the maps is to use detailed geometry information to run a streamline curvature code at several operating points and extract the maps from its output. Since this was not available for the T58 engine, the maps were approximated in the following manner.

The starting point for the maps is the characteristic map for the whole compressor that was obtained from the engine manufacturer. This was digitized to provide the corrected mass flow and total pressure ratio (the two dependent variables) for three different speeds and three different efficiencies (the independent variables). From this raw data, the generation of the stage-by-stage maps can be done in several different ways. We experimented with two of them as described below.

In the first method, the total pressure ratio pr, the corrected mass flow, and the efficiency η are assumed to be the same for all stages. Hence, for a given speed and efficiency, a total pressure ratio across an individual stage is calculated by taking the nth root of the total pressure ratio across the whole machine, where n is the number of stages. This is used along with the efficiency to calculate a total temperature ratio Tr across an individual stage from

$$Tr = [(pr^{(\gamma-1)/\gamma}-1)/\eta] + 1$$

where $\gamma = 1.4$, is the ratio of specific heats. In this way, for a given speed and efficiency, the mass flow, total pressure ratio, and total temperature ratio across each stage are obtained.

In the second method, the assumption is that the early stages of the compressor are more highly loaded than the latter stages. Let us denote the total pressure rise in the first five stages of the compressor to be prh, the total pressure rise in the last five stages of the compressor to be prl, and the total pressure ratio across the whole compressor to be prc. Then we have

$$(prh)^5 \, (prl)^5 = prc$$

A nominal value is arbitrarily assumed for prl, such as 1.0003, and the above equation solved for prh. Once the total pressure ratio across each stage is obtained, the total temperature ratio is obtained in the same way as in the first method. Note that if prh = prl, the second method reduces to the first method.

Once the mass flow, total pressure ratio, and total temperature ratio across each stage are obtained for each value of speed and efficiency by either of these methods, the DYNTECC preprocessor program STAGCHAR was used to generate an input file to PACFIT, the program that generates the characteristic fit file for DYNTECC. PACFIT is an interactive GUI based program that allows the user to check for characteristics that intersect. Unrealistic values of prl in the second method led to intersections of characteristic maps and were corrected. The stage characteristics give rise to the force and heat addition source terms that are used in the Euler momentum and energy equations, respectively.

COMPRESSOR SIMULATION USING LOSSY DUCTS

An even simpler simulation of the flow through a compressor can be obtained using the so-called "lossy" duct option within DYNTECC. In this option, the total temperature and pressure rise through each control volume can be input as parameters. By a proper selection of these parameters, it is possible to match the steady state flow field of a compressor.

For transient simulations, the source terms that would have produced the total pressure and temperature rise in steady flow are now added instantaneously to the momentum and energy equations. Dynamically, this option can be viewed as a compressor stage where the total temperature ratio and total pressure ratio remain constants, independent of mass flow and speed.

MODIFICATIONS TO DYNTECC

Relatively minor modifications to DYNTECC were required to be able to perform coupled simulations. The main modification consisted of implementing a data exchange procedure with NPARC that is described in the next section. In addition, the inflow boundary condition in DYNTECC is disabled during coupled simulation.

The coupled simulation is first run as a steady simulation so that the two codes settle down to a steady-state condition. Once this is achieved, the unsteady simulation, initiated by the bump collapse is carried out. Since it is difficult to lump these two steps into one (for example, the algorithm used on the NPARC side is different for the two steps), a restart option for the coupled simulation is necessary. NPARC already has a restart option. A restart option for DYNTECC was implemented by reading and writing the common blocks.

COUPLING PROCEDURE

GENERAL ISSUES

The basic method used to couple NPARC to DYNTECC is similar to the method used to couple two blocks of a multi-block code.[1] In this method, the conserved variables in the image cells of code A are obtained from interior cells of code B and vice-versa. The only new twist here is that the data transfer is 3-D to 1-D and 1-D to 3-D.

A mass-weighted average over the interior plane in NPARC is used to calculate values of the density, axial momentum and total energy required for the image cells of DYNTECC. Similarly, the same values from the interior cell of DYNTECC are applied as constant values over the image cells of NPARC, with the other two components of the conserved variables (those corresponding to the radial and circumferential components) being set to zero. Obviously, this method assumes that the flow is predominantly 1-D at the coupled plane. Since the units of variables are different in the two codes, some conversion factors were required to convert the data exchanged from one code to the other.

We remark that another method that has been used to couple codes is the so called boundary condition approach, where the boundary conditions of code A are satisfied by data from code B and vice versa. While this approach has its merits for steady flow (such as a faster convergence to steady state) it is not clear whether time accuracy will be maintained. Also, the boundary condition approach is not viable for cases where the flow at the interface can become supersonic.

DATA TRANSFER

For unsteady (time accurate) coupled simulations, data between NPARC and DYNTECC needs to be exchanged at the end of each time step. Since the codes are run separately and have widely different execution times per time step, synchronization of the two codes becomes an issue. In Ref. 1, the synchronization was handled by a script in the software used to couple the codes. Here, the synchronization is effected through file transfer and the Unix notion of a *pipe*. When a pipe is setup between two programs, the output of the first program forms the input to the second. Both pipes are initialized in both codes before the first time step. At the end of a time step, NPARC writes its averaged conserved variables into a pipe from which DYNTECC reads the data, and similarly DYNTECC writes to another pipe from which NPARC reads. Thus DYNTECC cannot proceed to time step n+1 unless NPARC has completed time step n and vice-versa. This method of data exchange works well in practice with little or no overhead (i.e., the time to exchange data was small compared to the program execution time per time step). The disadvantage of a pipe transfer is that there is a size limit to the data that can be transferred. In this case, the data is simply three real numbers so that this was not a problem.

VALIDATION

Two upstream perturbation cases were run to validate the method for coupling NPARC to DYNTECC. In both cases the collapsing bump was used to generate the perturbation. For the first validation case DYNTECC was used to simulate a continuation of the NPARC constant-area annular inlet. The duct Mach number was 0.17. The coupled simulation results are shown in Fig. 3. The static pressure time histories at NPARC station 4 and the first DYNTECC grid point (J=1) are seen to be essentially identical, except for high frequency oscillations observed in the NPARC data (beyond 9.5 msec). The oscillations are believed to be due to transverse waves set up by the bump collapse. These oscillations were also observed in the raw experimental data. The experimental data were filtered to remove frequencies above 2000 Hz due to engine noise and the transverse oscillations. All subsequent NPARC results have been filtered using the same procedure as the experimental data. Since the oscillations don't appear in the DYNTECC data, it would seem that the approach used to average the NPARC data from 3-D to 1-D effectively filtered them.

For purposes of comparison, a pulse strength Str is defined by the following equation

$$Str = \int_{t1}^{t2}(dp/p)dt = \int_{t1}^{t2}[(\bar{p}(t)-p)/p]dt$$

where $\hat{p}(t)$ and p are the instantaneous and initial values of the pressure at the particular axial location and the time limits of integration t1 and t2 are chosen to capture the (major) part of the pulse that is negative (e.g., values of t1 and t2 are about 7.5 msec and 8.7 msec for sta4). The pulse strength Str has units of msec. The pulse strengths at stations sta4 and J=1 are -2.39E-2 and -2.41E-2, respectively. The pulse at DYNTECC station J=7 (approximately the mid-compressor axial location) appears to be somewhat

attenuated. However, Str is -2.35E-2, only about 2 percent lower than the pulse strength on the NPARC side. This dissipation is thought to be due to the DYNTECC algorithm and it is felt that the pulse is accurately propagated across the NPARC/DYNTECC coupled interface.

For the second validation case DYNTECC was used to model the T58 converging flow path but without any compressor terms (i.e., there was no total pressure and temperature rise across the compressor region). In this case the duct Mach number was lowered to 0.04 to prevent the duct from becoming choked in the converging (T58 flow path) section. The compressor exit to inlet area ratio is 0.243. The incident pulse strength is slightly greater for this case than in Fig. 3 because of the different ambient conditions. The figure of merit for this validation case is the strength of the pulse reflected from the converging area relative to the incident pulse strength. Static pressure time histories for three sensor locations in the inlet duct (NPARC) are shown in Fig. 4. The incident and reflected pulse strengths were determined from the time history at NPARC sta3. The incident pulse occurs over the time range of about 7.4 to 8.6 msec, and its strength is –3.13E-2. The reflected pulse occurs over the time range of about 8.9 to 11.6 msec, and its strength is –2.15E-2. The ratio of reflected strength to incident strength is 0.687. Sajben[7] analyzed the reflection of acoustic pulses from compressor blades, and recently extended the analysis to include effects of change in area (unpublished to date). For an (abrupt) area change of 0.243 and an entrance Mach number of 0.04 Sajben's analysis predicts the ratio of reflected to incident pulse strengths to be 0.663, 3.5 percent less than the NPARC-DYNTECC result. We feel that the excellent agreement of the NPARC-DYNTECC result with Sajben's analysis further ensures that the NPARC-DYNTECC coupling method is valid.

DISCUSSION OF RESULTS

NPARC-DYNTECC ANALYSIS

Baseline case:

Coupled NPARC-DYNTECC simulations of the collapsing bump experiment were carried out for several different cases. In each case, the DYNTECC part of the simulation was changed to investigate a variety of conditions while the NPARC domain remained the same. The baseline case consisted of the T58 flow path and compressor stage maps with equal total pressure ratios across each stage (method 1 above). The total pressure and temperature ratios across the entire compressor were 2.40 and 1.39, respectively, and corresponded to the experimental test case with a duct Mach number of 0.17. This case will be referred to as the T58 flow path—linear loading case. Static pressure time histories in the inlet and engine are shown in Fig. 5.

The NPARC responses at sta1 and sta4 correspond to locations where experimental data were measured. The DYNTECC responses labeled as DTJ3, 7 and 14 correspond to grid locations J=3, 7 and 14 and are roughly at the entrance, midpoint and exit of the compressor. Fig. 5 shows the pulse amplitude being attenuated as it travels through the compressor. However, the values of Str at stations DTJ3 and DTJ7 are actually slightly greater than the incident pulse strength. While this cannot happen for isentropic ducts, such amplifications cannot be ruled out in the presence of source terms. A possible explanation is that reflections from successive source terms, as well as the converging flow path, may overlap the transmitted waves. Thus the pulse observed in the compressor could actually be a combination of transmitted and reflected waves. Unfortunately, experimental data do not exist to validate the static pressures computed within the compressor.

Comparison of other NPARC-DYNTECC results to baseline case:

Three other cases were run for comparison to the baseline case. The idea was to study the effects of the area variation and the source terms separately. In all cases the duct Mach number was 0.17 and the total pressure and temperature ratios across the compressor region were the same as for the baseline case. The particulars for each case are as follows:

1) Most of the total pressure rise through the engine is borne by the first five stages with the last five stages being essentially unloaded. This corresponds to the second method of generating characteristic maps described in DYNTECC stage characteristic maps section above and is referred to as the T58 flow path—front end loading case. Here the distribution of the total pressure rise through the engine is different as compared to the baseline case while the area distribution remains the same.

2) A constant area flow path, equal to the inlet annular area, was used with the baseline (linear) compressor pressure ratio terms. This case is referred to as the Constant area—linear loading case.

3) The DYNTECC lossy duct option was used to implement the same total pressure and temperature rise across the compressor as for the baseline case. The T58 flow path area was used. This case is referred to as the T58 flow path—lossy duct case.

These three cases are compared to the baseline case in Figs. 6 and 7. Fig. 6 shows a comparison of the reflected wave shapes, calculated at NPARC sta4, that occurred for the various cases. The reflected wave shape is obtained by translating the incident wave at sta1 to sta4 and then subtracting the translated wave from the combined incident/reflected wave to obtain the "net" wave. A procedure for doing this is described in more detail in Ref. 2. As can be seen the reflected wave shapes are pretty much the same for all cases except the lossy duct case.

The amplitude of the reflected wave is quite a bit larger for the front end loaded case as compared to the baseline. Unfortunately, this implies that the transient dynamics is quite sensitive to how the various stages are loaded, information that is usually difficult to obtain for a compressor. The pulse amplitude of the constant area case is only slightly smaller than the baseline case, despite the large area change in the latter, and this leads us to conclude that the stage characteristic source terms dominate the dynamic response.

The most striking difference in Fig.6 is between the lossy duct case and the baseline, where the reflected pulse amplitude is considerably smaller for the lossy duct. These two cases give steady state solutions that are almost identical but give dynamic solutions that are very different. This difference is not surprising since the source terms are implemented in completely different ways. It is also interesting that the shape of the reflected pulse is very similar to the second validation case of Fig. 4, where no source terms are present. From this we conclude that the source terms implemented in the lossy duct fashion have little effect on the dynamic response while source terms implemented via characteristic maps have a huge effect on the dynamic response.

Fig. 7 shows a comparison of static pressures in the compressor for each case with the baseline case. The T58 flow path—linear loading and constant area—linear loading cases are similar to the baseline but show somewhat greater attenuation as the pulse travels through the compressor. This would seem to imply that the area variation does not have a major effect when the compressor stage characteristic terms are present. (The reflected wave shapes in Fig. 6 also appear to support this conclusion.) The lossy duct case shows the pulse amplitude staying almost constant in strength as it travels through the compressor.

Simulation Times:

All computations were performed on an SGI R10000 multi-processor non-dedicated machine. The wall clock times for a complete run for the various simulations are as follows:

Simulation	Execution Time (sec)
Stand Alone NPARC	33251.4
Stand Alone DYNTECC	11.63
Coupled NPARC (serial)-DYNTECC	35560.8
Coupled NPARC (parallel) -DYNTECC	8298.6

As can be seen, the NPARC computation dominates. Thus, execution times are considerably reduced by parallel execution of NPARC. The elapsed times of the serial and parallel runs (with three blocks) are 10 and 2.5 hr, respectively. This compares with eight days and 12 hr for serial and parallel execution of NPARC-ADPAC, with the parallel computation run over 21 blocks. The difference between the execution time of the coupled simulation and the stand-alone NPARC simulation would be the communication overhead if these runs were carried out on a dedicated machine. As it is, it could well be due to different load factors during the two runs.

NPARC-DYNTECC ANALYSIS COMPARED TO EXPERIMENT

Selected NPARC-DYNTECC results are compared to the experimental results to give an indication of how well the DYNTECC code simulates the response of a multistage compressor to acoustic pulses. Fig. 8 shows time histories at two inlet duct locations (sta1 and sta4) for the baseline case compared to the experiment. The incident pulses, for the time range of about 6.0 to 7.2 msec, are in very good agreement. At station 4, the simulation time history indicates a larger reflection than the experiment although the agreement in the overall shape is not too bad. Fig. 9 shows a comparison of the T58 flow path—lossy duct case with the experiment. Again, the agreement for the incident pulses is very good. The agreement at station 4 is remarkably good both in shape and amplitude. Of all the analysis test cases this one appears to best replicate the experimental results.

From a controls perspective, the most important metrics for comparison are the shape and strength of the reflected wave. Fig. 10 shows the reflected wave determined at station 4 from various analyses compared to the experimental data. The strength ratio, defined as Str of the reflected pulse divided by Str of the incident pulse, is shown in parentheses for each case. The strength ratio for the NPARC-DYNTECC baseline case is 11 percent greater than that for the experimental result. The T58 flow path—lossy duct case mimics the experiment shape the best but its strength ratio is 30 percent lower than the experiment's.

From all these runs it appears that the shape of the reflected pulse is most affected by the flow path geometry. The result obtained from the previous NPARC-ADPAC (much more computationally expensive) simulation[1] predicts the initial part of the response quite well, but its overall shape and strength are not as good as the lossy duct case. This is consistent with the fact that ADPAC simulated just the first stage rotor of the T58 compressor and had no knowledge of the complete flow path (contraction) of the compressor. Although not shown in Fig. 10, a LAPIN 1-D simulation[1,7] of the experiment with the Paynter boundary condition[7] gives results that are very similar in shape to the NPARC-ADPAC case but had a larger strength ratio of 0.466. This simpler boundary condition approach has the advantage of much greater computational efficiency although it may not accurately represent the response of multiple blade rows, particularly in terms of reflected pulse shape. All of the simulation results are an improvement over the traditional exit boundary conditions such as constant pressure, velocity, or Mach number that would have strength ratios of −1, 1, and 0.934, respectively.

CONCLUDING REMARKS

The 3-D NPARC and 1-D DYNTECC CFD codes were successfully coupled to simulate the inlet and turbomachinery components, respectively, of the collapsing-bump compressor-interaction experiment conducted at the University of Cincinnati. Data were exchanged between codes by means of Unix pipes that added little overhead to the overall computation. The approach used to create 1-D variables from 3-D variables and vice versa was demonstrated to work very well, but is probably limited to cases where conditions at the coupled interface are predominately 1-D.

The main conclusion obtained from this work is that inlet-compressor interactions are not well captured by transient compressor codes that solve the 1-D Euler equations with source terms based on stage-by-stage characteristics. Although the strength of the reflected wave obtained by the analysis compared well with the experiment, the wave shape was not too good. Another (lossy duct) approach, wherein the flow path

geometry is modeled along with source terms representing the initial steady-state total pressure and temperature rise, gives results that compare well with experiment, especially in the shape of the reflected wave. With this approach, the reflected wave shapes obtained seem most sensitive to the flow path geometry while the reflected strengths seem most sensitive to the total pressure and temperature ratios. It appears that, at least for the compressor being simulated (T58), the flow path geometry plays an important role in determining the shape of the reflected wave. It may be that an additional (force) source term that accounts for reflection from the blade surface can be implemented in the momentum equation to produce more accurate results. In any case, all of the simulation methods discussed in the report are an improvement over exit boundary conditions, such as constant pressure, velocity, or Mach number, traditionally used to represent the compressor face boundary condition in CFD simulations of isolated inlet.

As mentioned in the introduction, the main advantage of using a 1-D code to simulate the compressor is that the entire compressor can be included in the simulation for little more than the cost of a stand alone inlet simulation. In addition, with parallel execution of the inlet code, turnaround times of a few hours are possible with this approach.

REFERENCES

1. Suresh, A., Townsend, S.E., Cole, G.L., Slater, J.W., and Chima, R., "Analysis of Inlet-Compressor Acoustic Interactions using Coupled CFD Codes," AIAA paper 98–0749; also NASA TM—1998-208839.
2. Freund, D., and Sajben, M., "Reflection of Large Amplitude Pulses from an Axial Flow Compressor," AIAA paper 98–0749, Jul. (1997).
3. Chung, J., Slater, J., Suresh, A., and Townsend, S., "NPARC v3.1 User's Guide: A Companion to the NPARC v3.0 User's Guide," NASA TM—1999-209058, March, 1999.
4. Hale, A.A., and Davis, M.W., Jr., "Dynamic Turbine Engine Compressor Code DYNTECC—Theory and Capabilities," AIAA paper 92–3190, July (1992).
5. Owen, K.A., and Davis, M.W., Jr., "Modeling the Dynamic behavior of an Axial-Centrifugal Compression System," AIAA paper 94–2802, June (1994).
6. Sajben, Miklos, "Acoustic, Vorticity, and Entropy Waves Created by Acoustic Pulses Incident on a Moving Blade Row," paper IS–7085, September, 1999.
7. Paynter, G.C., Clark, L.T., and Cole, G.C., "Modeling the Response from a Cascadeto an Upstream Acoustic Disturbance," AIAA paper 98–0953, Jan. (1998).
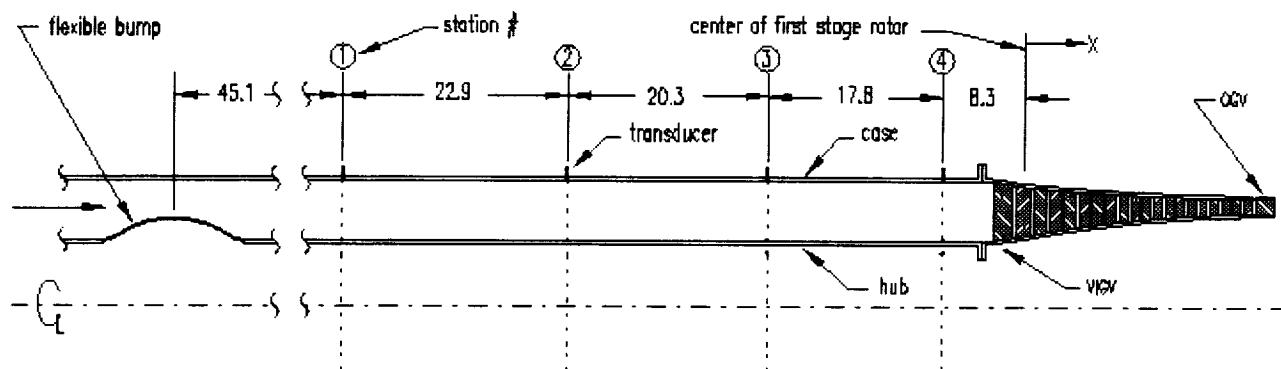
Fig. 1 - Schematic of U. Cincinnati inlet-engine acoustic pulse experiment and pressure sensor locations (dimensions in centimeters).
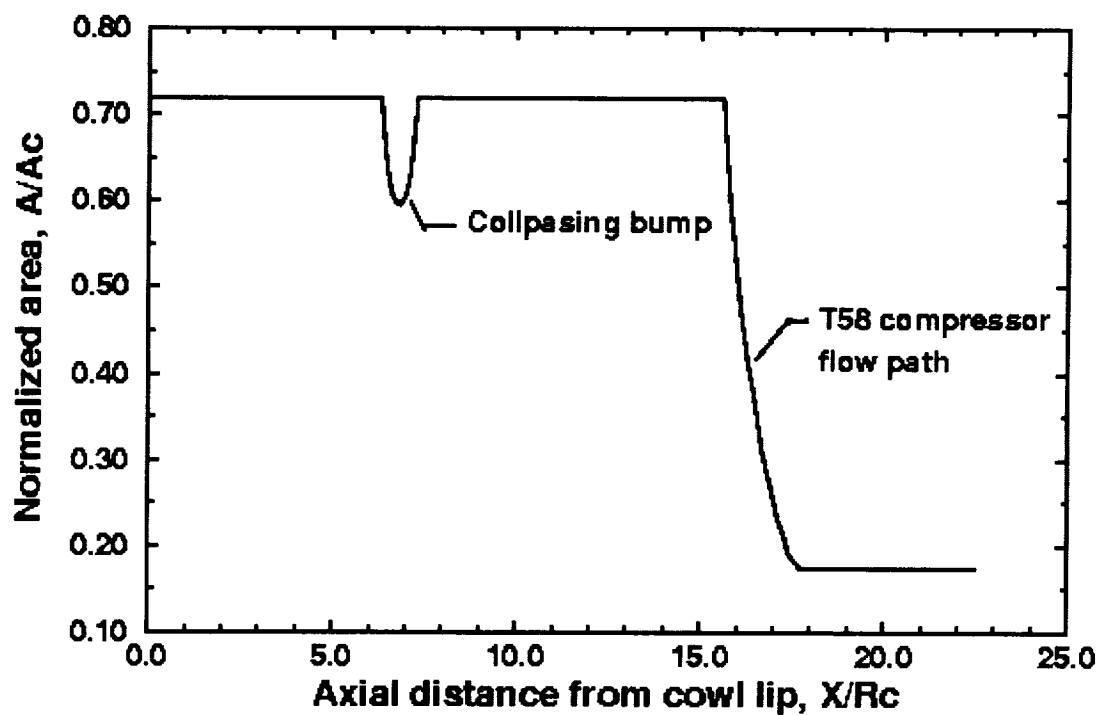

Fig. 2 – Area distribution of inlet duct and T58 compressor flow path (collapsing bump inflated).
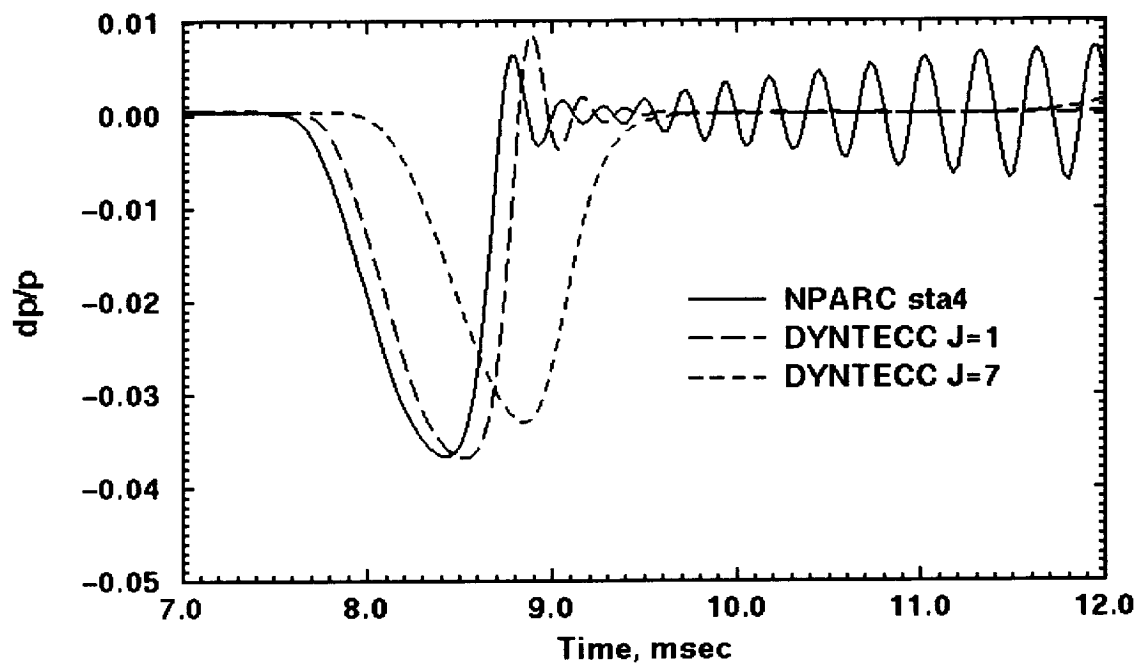
Fig. 3 – Static pressure time histories for constant area coupled-code validation case.
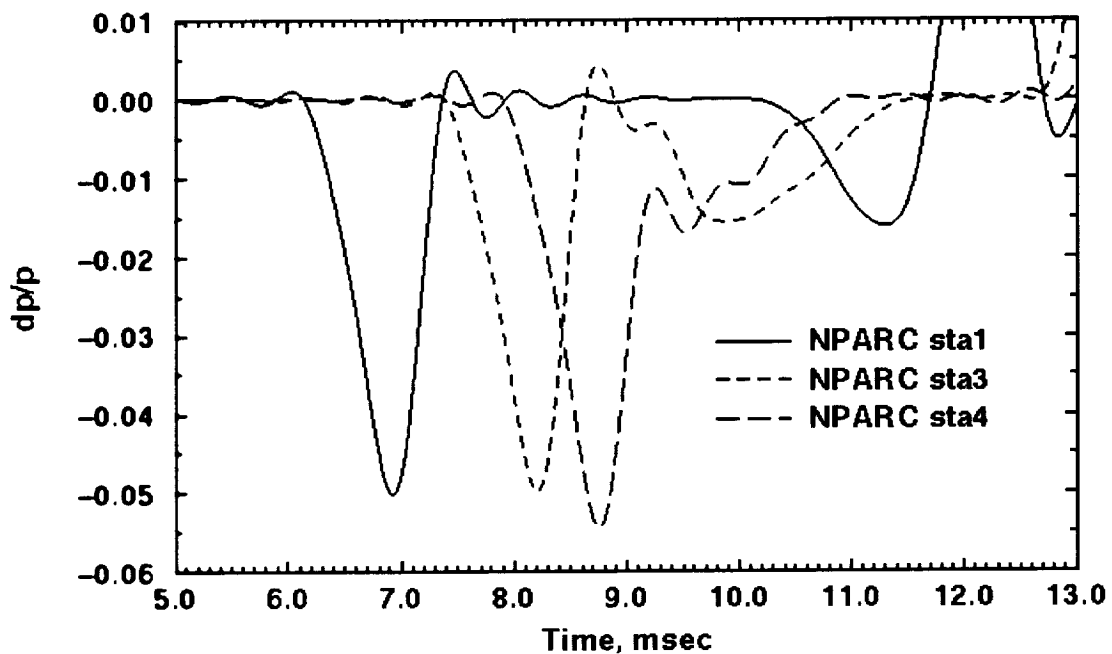

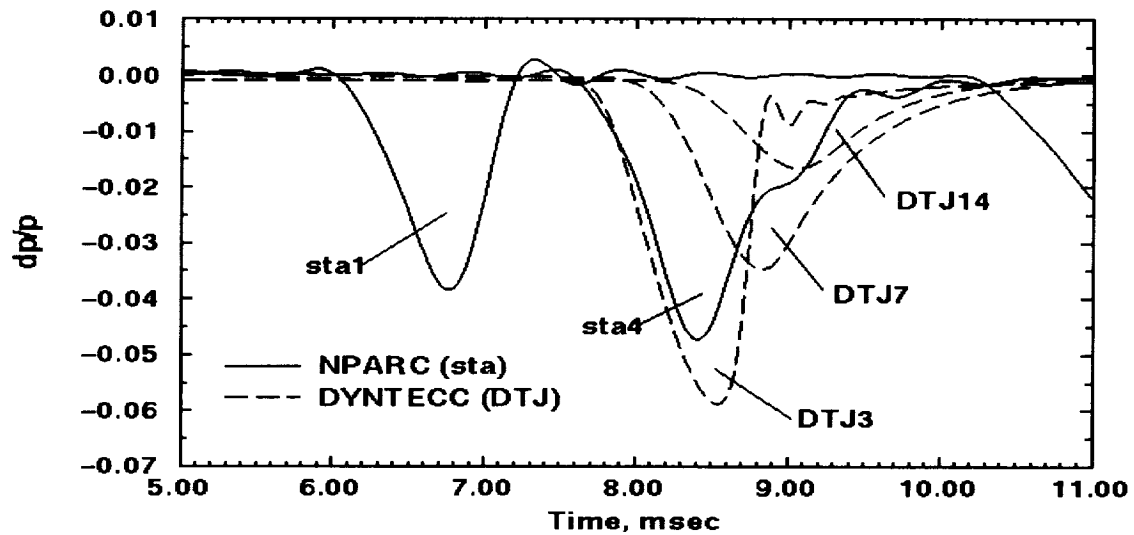Fig. 4 - Static pressure time histories for T58 compressor flow path coupled-code validation case.

Fig. 5 – Static pressure time histories for T58 compressor flow path with uniform total-pressure (linear loading) across stages (baseline case).
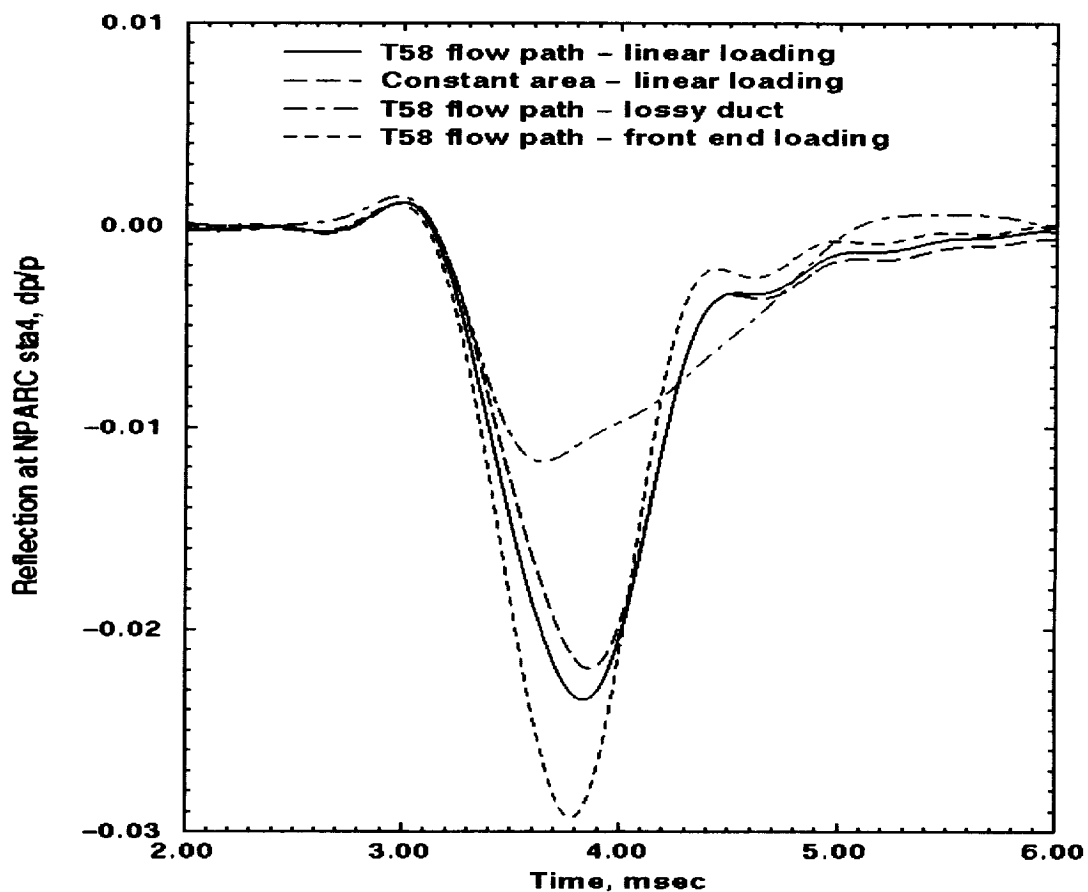
Fig. 6 – Comparison of "net" reflected pulse measured at inlet station 4 for coupled NPARC-DYNTECC solutions to various flow path and compressor loading cases.
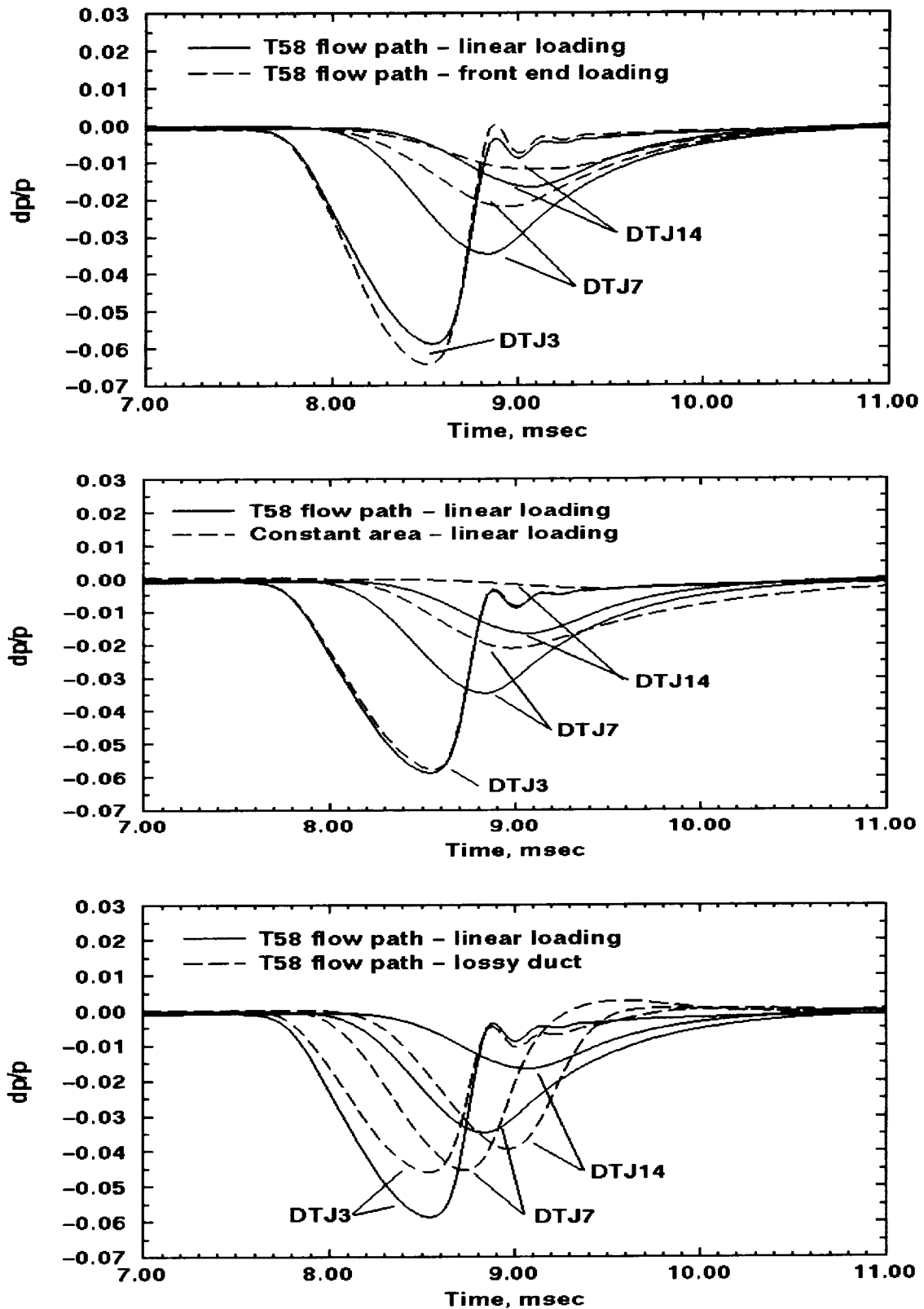
Fig. 7 – Static pressure time histories in T58 compression region for various cases compared to T58 flow path – linear loading (baseline) case.
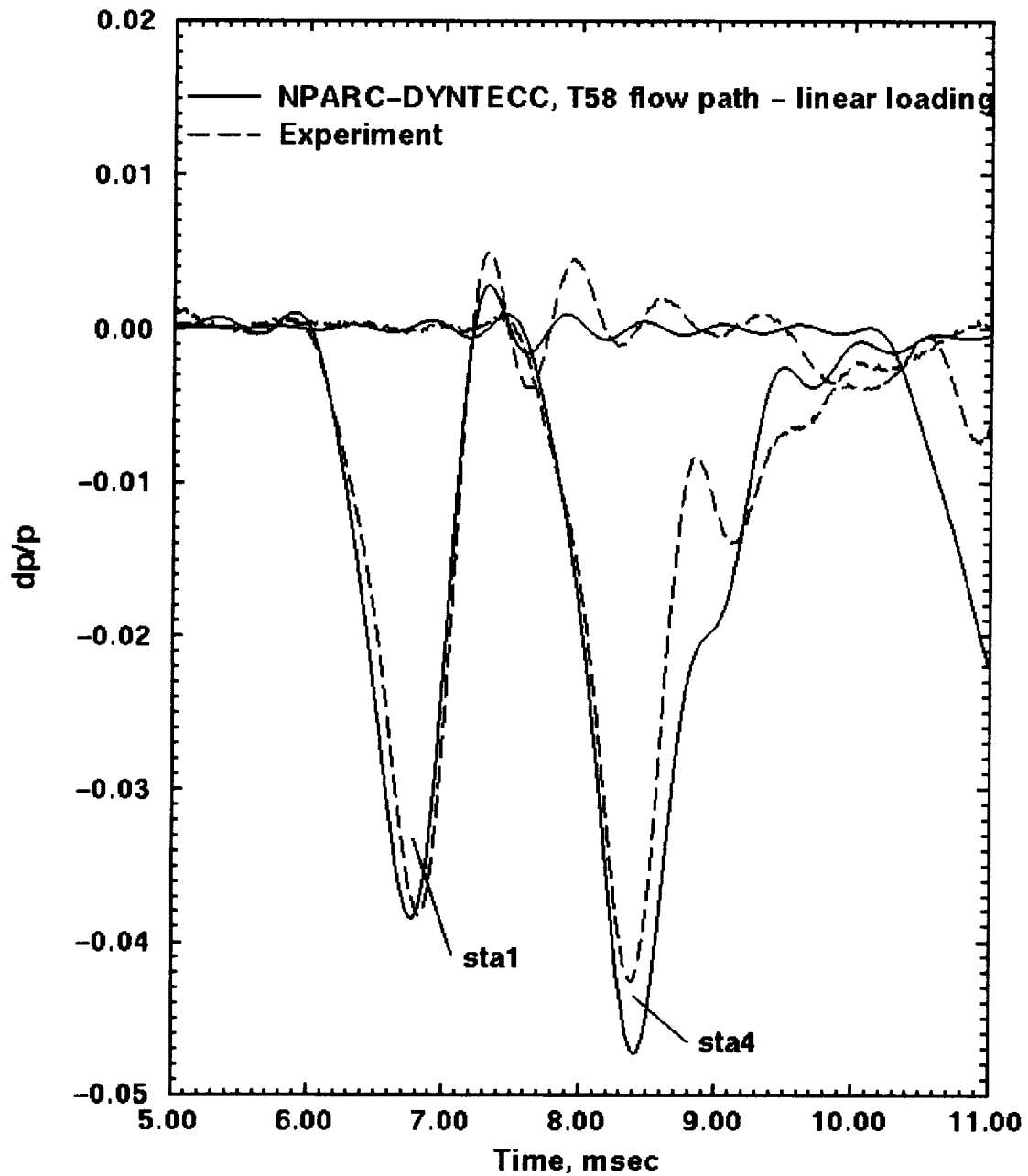
Fig. 8 – Static pressure time histories in inlet region for T58 flow path – linear loading (baseline) case compared to U. Cincinnati experimental data.
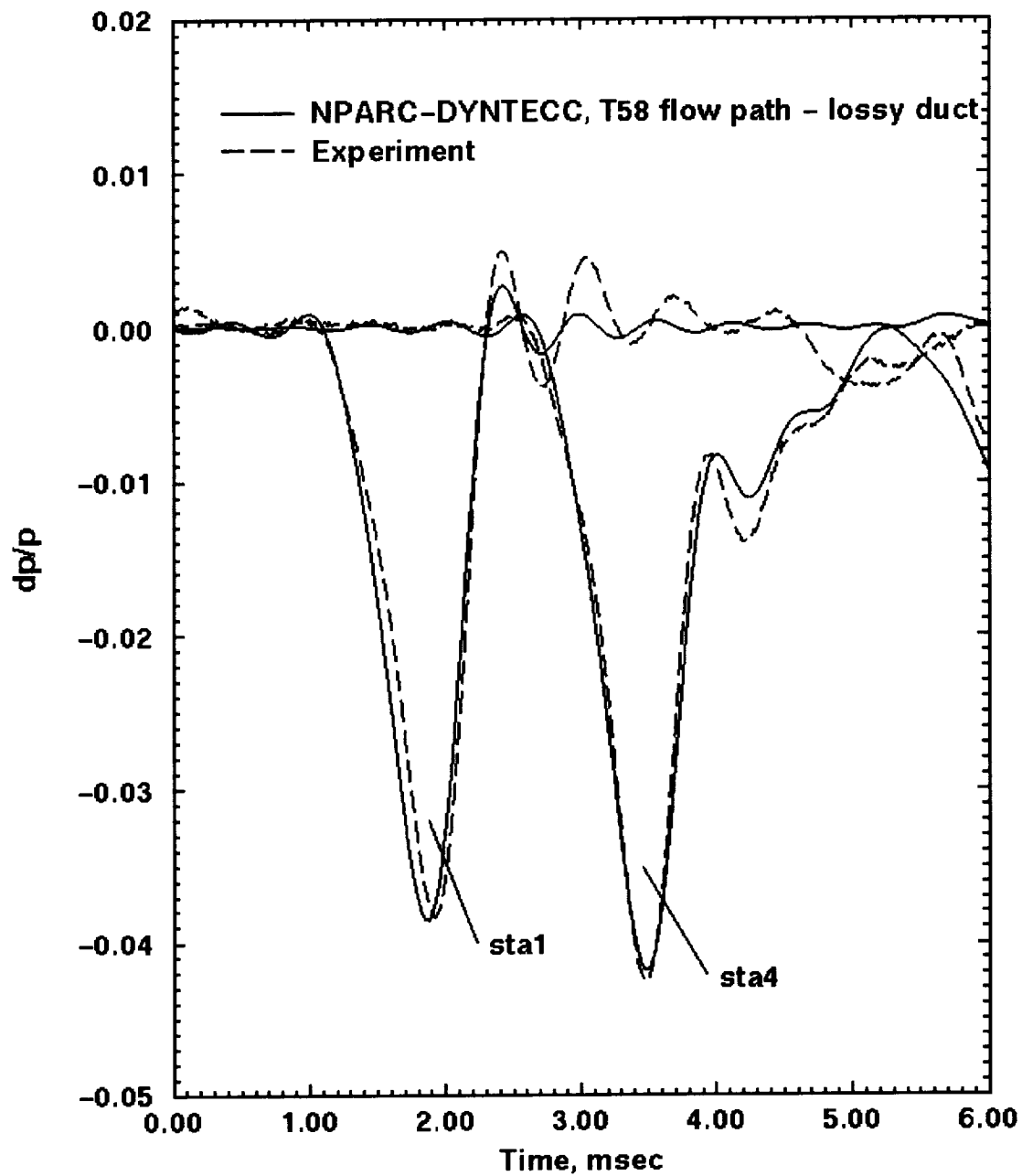
Fig. 9 – Static pressure time histories in inlet region for T58 flow path – lossy duct case compared to U. Cincinnati experimental data.
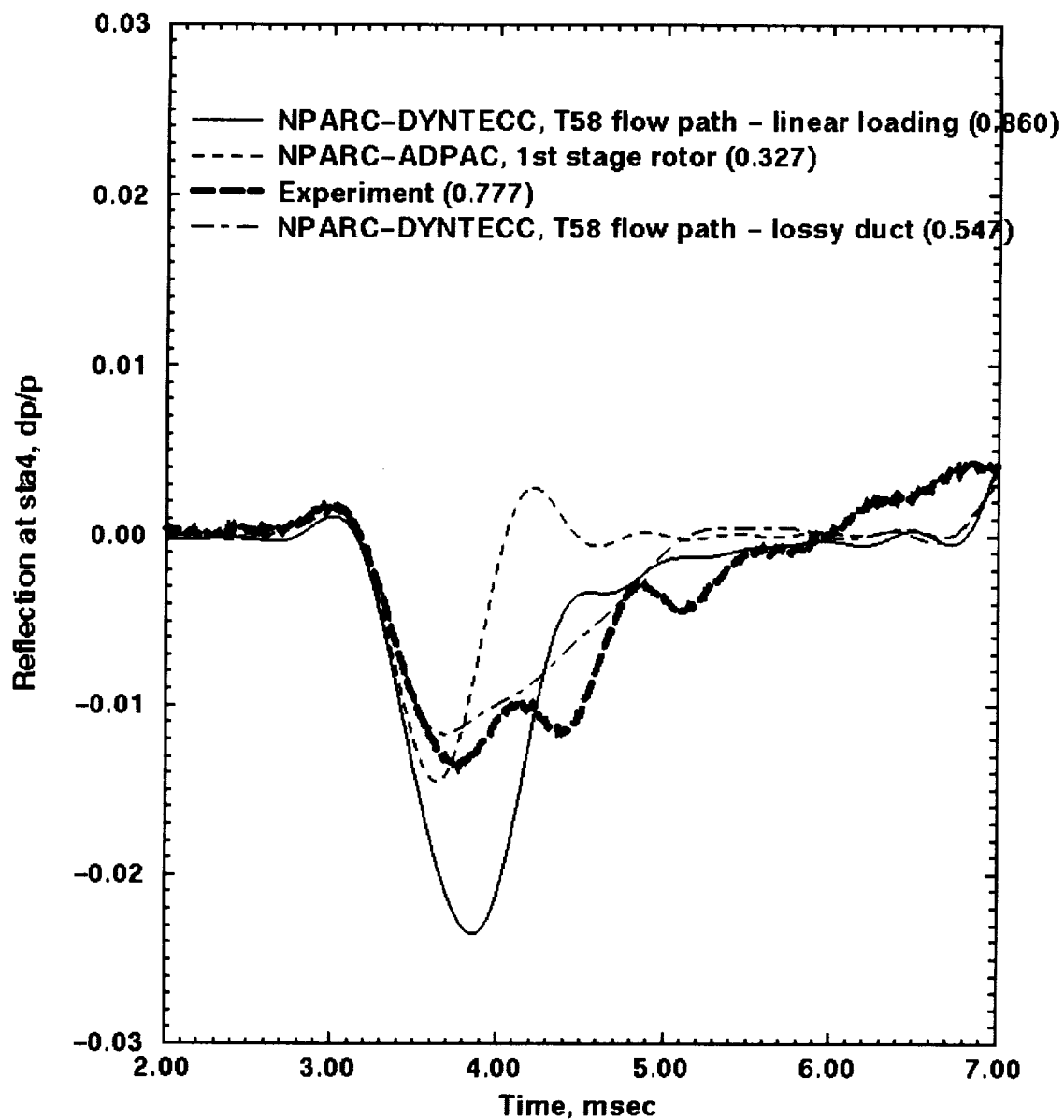
Fig. 10 – "Net" reflected pulse measured at inlet station 4 for coupled NPARC-DYNTECC solutions compared to U. Cincinnati experimental data and coupled NPARC-ADPAC solution. Values in parentheses are ratio of reflected pulse amplitude (time integral of dp/p) to incident pulse amplitude.

REPORT DOCUMENTATION PAGE

Public reporting burden for this collection of information is estimated to average 1 hour per response, including the time for reviewing instructions, searching existing data sources, gathering and maintaining the data needed, and completing and reviewing the collection of information. Send comments regarding this burden estimate or any other aspect of this collection of information, including suggestions for reducing this burden, to Washington Headquarters Services, Directorate for Information Operations and Reports, 1215 Jefferson Davis Highway, Suite 1204, Arlington, VA 22202-4302, and to the Office of Management and Budget, Paperwork Reduction Project (0704-0188), Washington, DC 20503.

1. AGENCY USE ONLY (Leave blank)	2. REPORT DATE	3. REPORT TYPE AND DATES COVERED
	September 2000	Technical Memorandum

4. TITLE AND SUBTITLE

Unsteady Analysis of Inlet-Compressor Acoustic Interactions Using Coupled 3-D and 1-D CFD Codes

5. FUNDING NUMBERS

WU–509–10–11–00

6. AUTHOR(S)

A. Suresh and G.L. Cole

7. PERFORMING ORGANIZATION NAME(S) AND ADDRESS(ES)

National Aeronautics and Space Administration
John H. Glenn Research Center at Lewis Field
Cleveland, Ohio 44135–3191

8. PERFORMING ORGANIZATION REPORT NUMBER

E–12367

9. SPONSORING/MONITORING AGENCY NAME(S) AND ADDRESS(ES)

National Aeronautics and Space Administration
Washington, DC 20546–0001

10. SPONSORING/MONITORING AGENCY REPORT NUMBER

NASA TM—2000-210247

11. SUPPLEMENTARY NOTES

12a. DISTRIBUTION/AVAILABILITY STATEMENT

Unclassified - Unlimited
Subject Categories: 07 and 02   Distribution: Nonstandard

This publication is available from the NASA Center for AeroSpace Information, (301) 621–0390.

12b. DISTRIBUTION CODE

13. ABSTRACT (Maximum 200 words)

It is well known that the dynamic response of a mixed compression supersonic inlet is very sensitive to the boundary condition imposed at the subsonic exit (engine face) of the inlet. In previous work, a 3-D computational fluid dynamics (CFD) inlet code (NPARC) was coupled at the engine face to a 3-D turbomachinery code (ADPAC) simulating an isolated rotor and the coupled simulation used to study the unsteady response of the inlet. The main problem with this approach is that the high fidelity turbomachinery simulation becomes prohibitively expensive as more stages are included in the simulation. In this paper, an alternative approach is explored, wherein the inlet code is coupled to a lesser fidelity 1-D transient compressor code (DYNTECC) which simulates the whole compressor. The specific application chosen for this evaluation is the collapsing bump experiment performed at the University of Cincinnati, wherein reflections of a large-amplitude acoustic pulse from a compressor were measured. The metrics for comparison are the pulse strength (time integral of the pulse amplitude) and wave form (shape). When the compressor is modeled by stage characteristics the computed strength is about 10% greater than that for the experiment, but the wave shapes are in poor agreement. An alternate approach that uses a fixed rise in duct total pressure and temperature (so-called "lossy" duct) to simulate a compressor gives good pulse shapes but the strength is about 30 percent low.

14. SUBJECT TERMS

Inlet compressor; Unstart; Code coupling

15. NUMBER OF PAGES

22

16. PRICE CODE

A03

17. SECURITY CLASSIFICATION OF REPORT	18. SECURITY CLASSIFICATION OF THIS PAGE	19. SECURITY CLASSIFICATION OF ABSTRACT	20. LIMITATION OF ABSTRACT
Unclassified	Unclassified	Unclassified	